SUPPLEMENTAL DATA

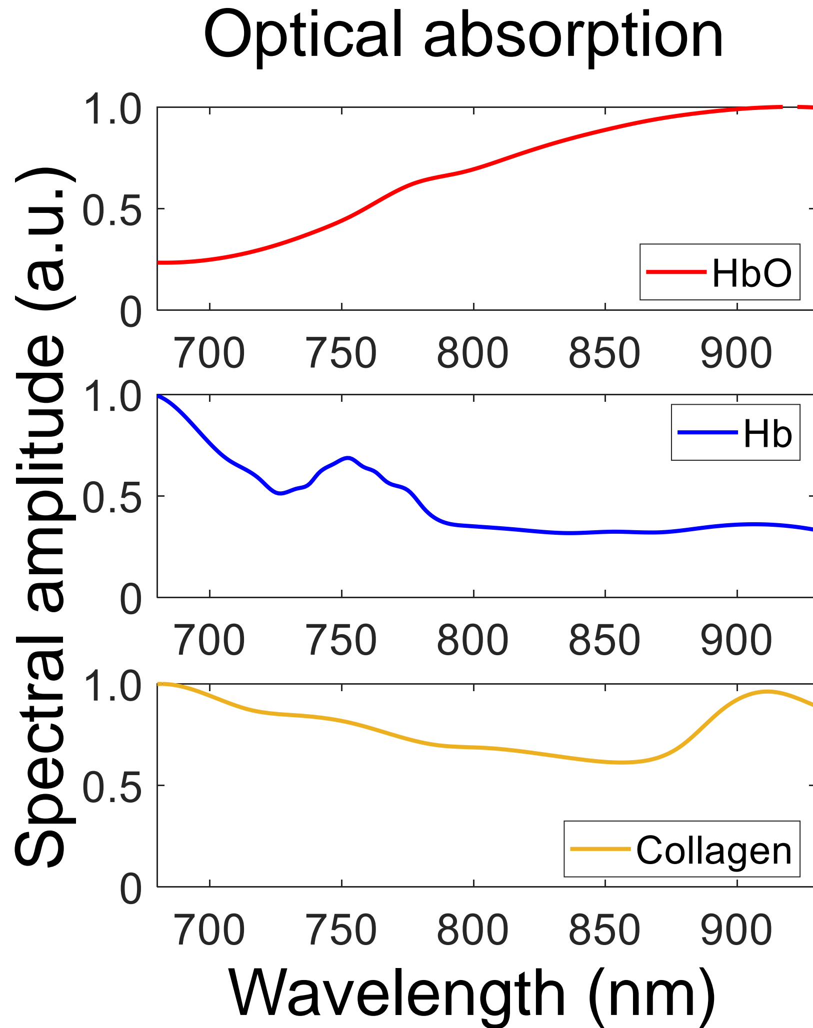

Supplemental Figure 1: Optical absorption as a function of illumination wavelength for the dominant chromophores in kidney (HbO = oxyhemoglobin; Hb = deoxyhemoglobin; collagen).
Extinction coefficient data retrieved from (63) and (64).

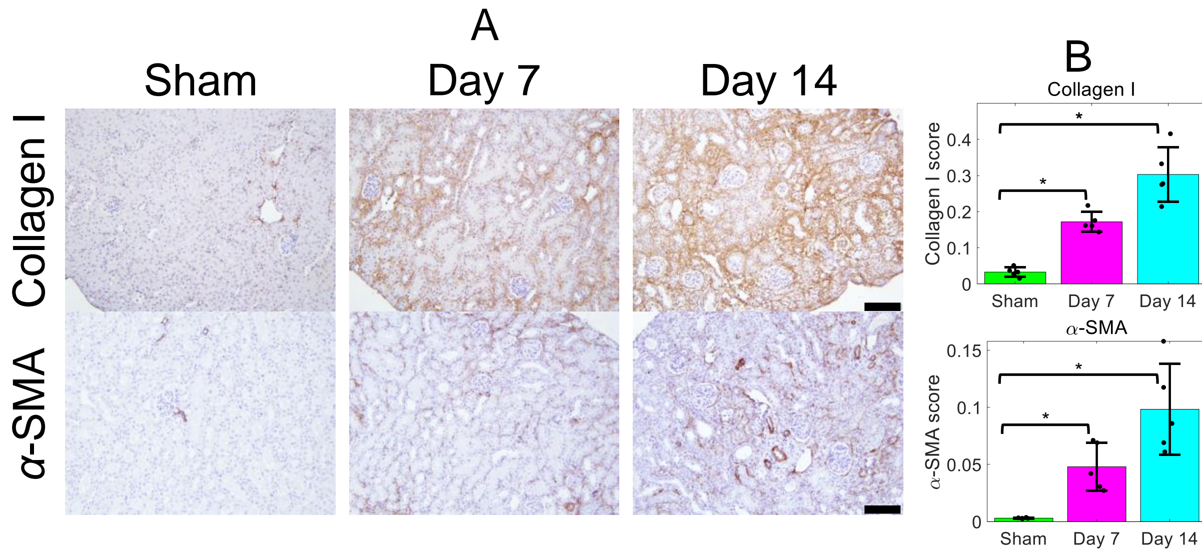

Supplemental Figure 2: Renal fibrosis progresses with time following unilateral ureteral obstruction (UUO).

(**A**) Representative images following staining with antibodies directed against type 1 collagen and alpha-smooth muscle actin (α-SMA) as a function of time post-UUO surgery. The scale bar denotes 100 μm and it applies to all images. (**B**) Quantification of type I collagen and α-SMA staining following UUO-surgery. Between group comparisons were performed with one-way ANOVA and post-hoc Tukey's analysis (* denotes statistical significance with $p < 0.05$ for relative to sham with n = 5 kidneys measured at every experimental timepoint). For type I collagen staining $p = 1 \times 10^{-5}$ for sham vs. day 7 post-UUO animals. $p = 1 \times 10^{-6}$ for sham vs day 14 post-UUO animals. For α-SMA staining $p = 1 \times 10^{-6}$ for sham vs. day 7 post-UUO animals. $p = 1 \times 10^{-5}$ for sham vs day 14 post-UUO animals.

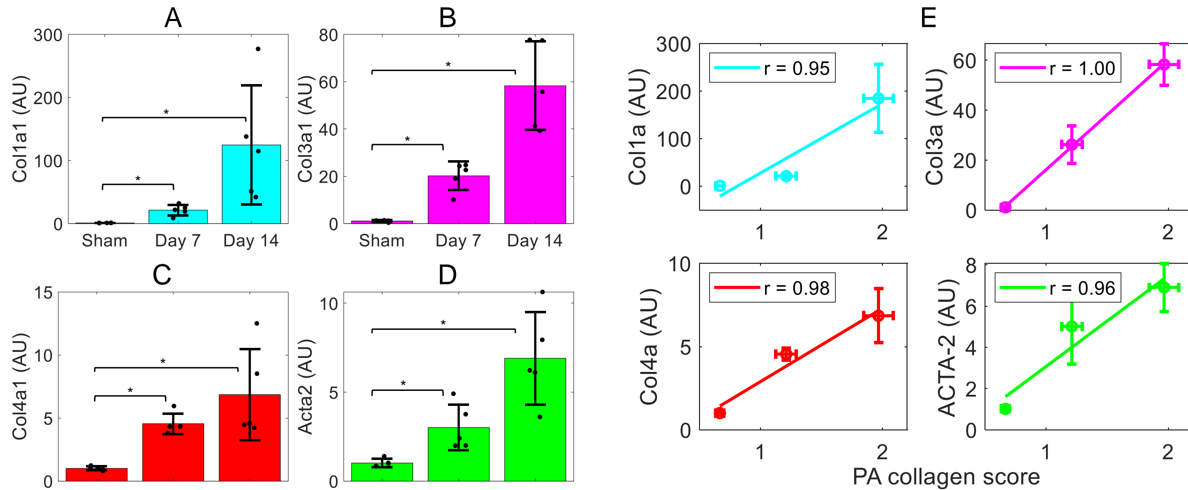

Supplemental Figure 3: PA-derived collagen measurements correlate strongly with mRNA levels of fibrosis-associated genes.

mRNA was isolated from kidney tissue collected from mice at 7 and 14 days post-UUO surgery or 14 days post-sham surgery, and reverse transcribed to cDNA. The levels of the following fibrosis-associated genes were measured: (**A**) Col1a1, (**B**) Col3a1, (**C**) Col4a1, and (**D**) Acta2. Between group comparisons were performed with one-way ANOVA and post-hoc Tukey's analysis (* denotes statistical significance with $p < 0.05$ for relative to sham with n = 5 kidneys measured at each timepoint). The p values for Col1a1, Col3a1, Col4a1 and Acta2 for sham vs day 7 post-UUO animals are $p = 0.0004$, 0.005, 0.000001 and 0.03, respectively and for sham vs day 14 post-UUO animals they are $p = 0.016$, 0.00007, 0.004 and 0.0005, respectively. (**E**) PA-derived collagen scores were then correlated with mRNA levels of each of these genes using Pearson correlation coefficient analysis, producing Pearson r values of 0.95 – 1.0 ($p = 0.02$ for Col1a1, $p = 0.002$ for Col3a1, $p = 0.01$ for Col4a1, $p = 0.02$ for Acta2). Abbreviations: AU, arbitrary units.

Collagen type	Primer sequence
Mouse Col1a1 forward	GAGAACCAGCAGAGCCA
Mouse Col1a1 reverse	GAACAAGGTGACAGAGGCATA
Mouse Col3a1 forward	GAAAGGATGGAGAGTCAGGAA
Mouse Col3a1 reverse	CATTGCGTCCATCAAAGCC
Mouse Col4a1 forward	TTCTCCCTTTTGTCCCTTCAC
Mouse Col4a1 reverse	GCTTCTGCTGCTCTTCGC
Mouse Acta2 forward	CACTGAACCCTAAGGCCAAC
Mouse Acta2 reverse	GAGTCCAGCACAATACCAGTT
Mouse Gapdh forward	CACCATCCGGGTTCCTATAAAT
Mouse Gapdh reverse	TGGCACTGCACAAGAAGAT

Supplemental Table 1: qPCR primer sequences.

SUPPLEMENTAL METHODS

Photoacoustic spectral unmixing

A. Optimal wavelength selection

The quantification of collagen (the dominant protein in fibrosis) in the presence of oxy and deoxyhemoglobin (the dominant chromophores of most biological tissues) requires the selection of optical wavelengths that allow for the most stable spectral unmixing solutions. These optimal wavelengths were identified by minimizing the variance inflation factor (VIF) from the extinction coefficients for each of the three dominant chromophores (collagen, deoxyhemoglobin and oxyhemoglobin). The VIF is a metric that can quantify the stability of the solution of a linear system of equations that consist of the extinction coefficients of each chromophores at wavelength (this is required for the spectral unmixing solution, details below) (60). The collinearity of the vectors comprising the matrix of known extinction coefficients typically results in high VIFs, therefore requiring the minimization of the VIF.

The selection of the most optimal wavelengths for unmixing was achieved by using the extinction coefficients for collagen, deoxyhemoglobin and oxyhemoglobin in the 680-930 nm range. Three random wavelengths were selected in order to create an initial 3×3 matrix of the extinction coefficients of each chromophore at the respective wavelengths. This matrix was multiplied by its transpose and the inverse of the product was computed. The diagonal of the inverted matrix represents the VIFs of that matrix. This procedure was repeated by performing a 1 nm sweep across the wavelength range (680-930 nm) in order to determine the most optimal wavelengths. The outputted VIFs at every set of wavelengths were minimized by sorting the VIFs in increasing order

across all wavelength permutations. This procedure determined that the extinction coefficients at 680, 725 and 755 nm yield the most stable spectral unmixing solution.

B. Photoacoustic image reconstruction

Once the PA data at each respective wavelength was saved in the system, the radiofrequency (RF) data was exported offline. For the VevoLAZR-X system, the data is exported as pre-beamformed. The first step in the algorithm involved taking into account the time delays for all 256 channels. This was achieved with a conventional delay-and-sum beamforming algorithm which compensated the relative delays on a 64 element sub-aperture and summed the signal contributions (57). For 2D PA scanning was performed, the PA data was averaged across all 2D frames acquired.

Once the beamformed PA data was obtained for all the frames acquired (for 2D and 3D scanning), it was compensated for the wavelength-dependent fluctuations in laser energy. This was achieved by dividing the beamformed PA matrix by the energy of the laser at that given frame. To form a 2D PA image, the amplitude of each pixel was calculated by performing the Hilbert Transform across each of the 256 transducer channels. To display the image, logarithmic compression was performed by taking the $20 \times \log_{10}$ of the amplitude matrix.

C. Linear spectral unmixing

The PA amplitude matrix acquired at each of the optimal wavelengths is the input to the spectral unmixing algorithm (23). This amplitude matrix was thresholded using Otsu’s method in order to filter out the noise present in the images (65). The unmixing was performed using the normalized extinction coefficient plots (Supplementary Figure 1) for each of the three dominant chromophores

(64). The PA amplitude matrices at each wavelength were used to solve the linear system of extinction coefficients using the least-squares method. Restrictions to the solution were implemented in order to improve the chromophore concentration quantification by limiting the output of the algorithm between 0% and 100% to avoid non-physical solutions (ex. oxygen saturation < 0%) and requiring that the concentrations of all chromophores together sum to 100%.